JOURNAL OF APPLIED ELECTROCHEMISTRY 10 (1980) 511–525

The electrodeposition of lead dioxide on titanium

D. GILROY, R. STEVENS

Electricity Council Research Centre, Capenhurst, Chester, UK

Received 24 August 1979

The initial stages of the potentiostatic deposition of lead dioxide from acidic lead nitrate solution, onto titanium wires, have been followed. The observed current transients and size distributions of the nuclei have been related to available theories of electrocrystallization by assuming a stochastic growth process. The inhibiting effects of fluoride ions are emphasized.

1. Introduction

Lead anodes, frequently used in electrowinning applications, suffer the disadvantage that the outer lead dioxide layer is continually removed by shedding or dissolution. As well as the obvious effect this may have on the electrode lifetime, contamination of the cathode can also result. It is economically advantageous in many cases to develop an alternative to precious metal containing dimensionally stable anodes by attempting to use lead dioxide deposited onto an inert substrate. This approach may already be commercially practised, but only to a limited extent, in the production of chlorine, hypochlorite and perchlorate.

When employed as an oxygen-evolving electrode, lead dioxide has shedding problems caused by, or followed by, passivation or destruction of the substrate, which may become severe. Kelsall [1] has reviewed the applications and the many methods published in the patent literature, and elsewhere, for the preparation of lead dioxide anodes. The most commonly used substrates are titanium and graphite, although Fleischmann and co-workers [2, 3] have studied the nucleation at platinum as a model process to illustrate various aspects of electrocrystallization. The present work, which forms part of a programme on the PbO_2/Ti system is concerned with the initial stages of electrodeposition of lead dioxide from acidic nitrate solutions.

2. Experimental

2.1. *Solutions*

Throughout this work PbO_2 was electrodeposited from 0.5 M $Pb(NO_3)_2$, 0.1 M HNO_3 solutions, containing additions of NaF up to the saturation value of 4.5×10^{-2} M (approximately), at which point lead fluoride precipitates. AnalaR chemicals (B.D.H. Ltd) were dissolved in triply distilled water. When fluoride was present, the nitrate and fluoride containing parts of the mixture were usually de-oxygenated separately by argon bubbling, and the final solution obtained by subsequent mixing. This procedure was adopted to prevent the possible loss to the gas stream of fluoride as HF, which is a significant component at low pH. The experimental temperature was within the range 19.5–21.8° C.

2.2. *Cell and electrodes*

An all-glass cell with outlets for the electrodes, the purging gases, and the sodium fluoride solution burette was constructed. The platinum gauze counter electrode was located in the main compartment together with the working electrode. A separate internal compartment with a Luggin capillary was provided for the reference electrode of PbO_2 plated on platinum gauze. The total solution volume was 200 cm^3.

The working electrode, which was designed for ease of removal and subsequent examination, is shown in Fig. 1. 1 mm diameter titanium wire (Goodfellow Metals Limited) of > 99.6% purity was straightened by stretching, and short lengths were inserted into 1 mm bore quartz sleeves, sealed at one end with araldite, and welded to the electrical lead-throughs. The working section of titanium wire, about 20 mm long, was prepared by blasting with 50 μm alumina particles followed by ultra-sonic cleaning in propanol. The procedure has been described by King [4]. The electrodes were left to dry in air and stored before use. Prior

0021–891X/80/040511–15$03.50/0

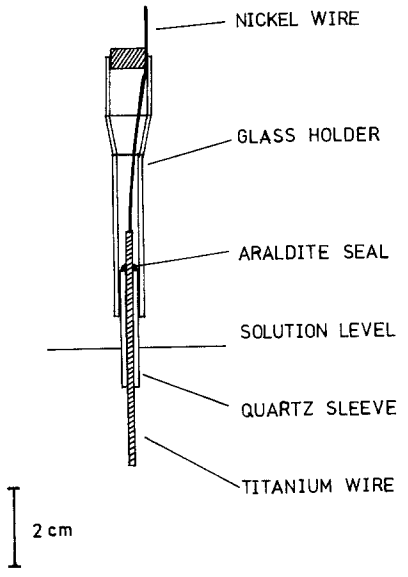

Fig. 1. Construction of electrodes.

to an experiment an individual electrode was inserted into a glass holder and placed in the cell.

2.3. *Experimental procedure*

After the components had been de-oxygenated and mixed, argon was blown over the surface of the solution for the duration of the experiment. An electrode was introduced into the cell, and left on open circuit for a specified period, during which it could be rotated into position near the Luggin capillary, and electrical connections made. The electrode was then brought under potentiostatic control and subjected to a multi-step programme of the type shown in Fig. 2. Conventional circuitry, with current recording along the appropriate potential steps, was used. The initial period at 0 V eliminates much of the double layer charging in the transition from open circuit to the growth stages. After an experiment the programme returned to 0 V, the potentiostat was switched off, and the electrode rapidly removed from the cell, and first rinsed in distilled water and then in methanol. After drying in air the holder and the electrical lead were removed and the electrode stored before further examination.

2.4. *Microscopy*

The working length of the titanium wire was cut off and attached to an aluminium specimen stub with a silver based electrically conducting adhesive. During the mounting and insertion into the scanning electron microscope (Cambridge 180), care was taken with the alignment procedures to ensure that the three-dimensional geometry was known, so that spatial corrections could be made when calculating the nuclei density.

Electron micrographs of the lead dioxide nuclei were taken at different magnifications, usually in the range x 300–3000, on areas that had projected surfaces perpendicular to the incident electron beam. Several areas on a given wire were examined to ensure that representative samples were obtained.

Sections of the micrographs were divided into known areas and the number, N, and diameters, d, of lead dioxide nuclei in an area were measured using a graduated optical lens loupe. Usually $70 < N < 150$. When calculating the surface den-

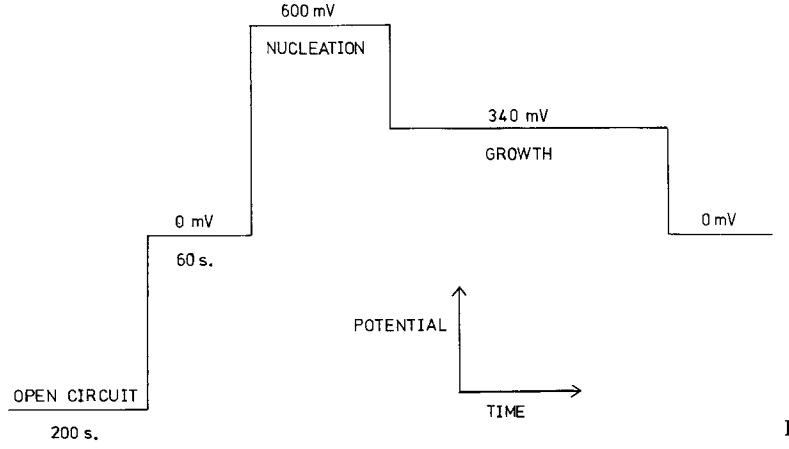

Fig. 2. Potential–time programme.

sity of nuclei, corrections were made to account for the tilt of the specimen, but not for the curved surface of the titanium wire, since the drawing characteristics did not produce perfectly cylindrical geometry. In situations where nuclei had overlapped, the diameters of the individual spheres were obtained whenever possible.

3. Results

For the majority of specimens a current transient and a size distribution for nuclei at the end of the polarization time were obtained. The current measurements are presented as functions of t, t^2, or t^3, as appropriate. The N nuclei measured on a particular specimen are numbered $1, 2, 3, \ldots, n_d, \ldots, N$ in order of increasing diameter, d, and the size distribution was shown by plotting n_d/N as a function of d. In preliminary experiments no significant effects of variations in the specimen age, (between 2 and 60 h) and in the pre-growth steps of the potential programme, in fluoride free solution, were found.

3.1. *Fluoride free solutions*

3.1.1. Potentiostatic transients. Throughout this work a growth potential of 340 mV with respect to the lead dioxide reference electrode was generally used. At this potential the time taken for the initially formed nuclei to overlap was conveniently of the order of 300 s. A typical current transient is shown in Fig. 3, and the initial section is plotted in Fig. 4 as a function of t^3 and t^2. The I versus t^2 plot is approximately linear. Introducing a nucleation step at 600 mV, for various times, gave the results of Fig. 5, which do not conform to linear i–t^2 behaviour.

Changing the growth potential produces the variations shown in Fig. 6. A short nucleation pulse (0.2 s at 600 mV) was used to ensure that measurable currents were observed at the lower potentials. On spec 59 and 60, where growth was quite slow, linear i–t^2 plots were obtained; an example is given in Fig. 7.

3.1.2. Size distributions of nuclei. The measured distributions corresponding to the above situations are given in Figs. 8–10. The specimens are identified by numbers so that the appropriate current transient may be referred to. Fig. 8 depicts the time variation of the nuclei sizes during potentiostatic growth at 340 mV. Overlap of individual nuclei and their intergrowth soon becomes pronounced under these conditions. Fig. 9 corresponds to the experiments of Fig. 5 with a nucleation step followed by 30 s growth at 340 mV, and Fig. 10 may be considered in conjunction with Fig. 6.

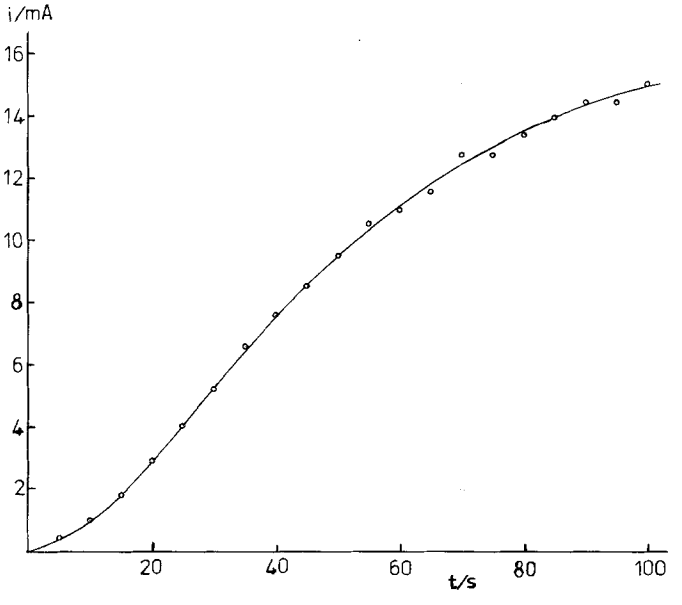

Fig. 3. Current–time transient for growth at 340 mV ($[F^-] = 0$).

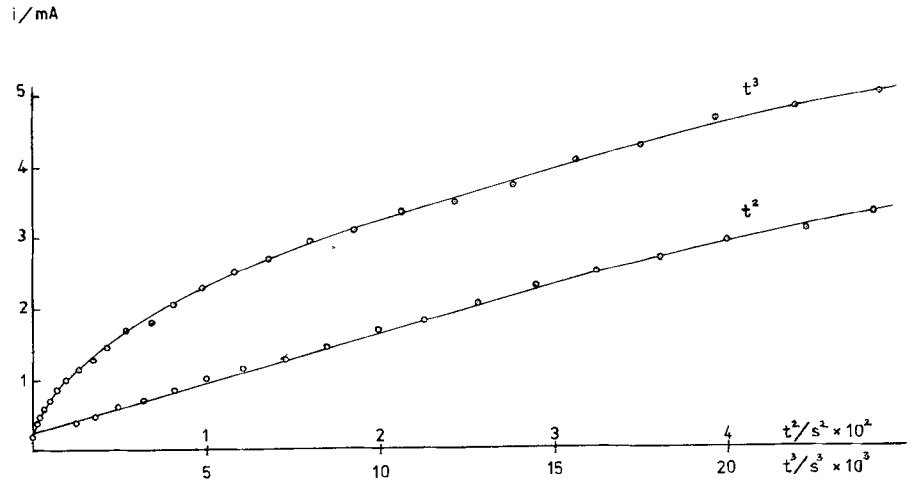

Fig. 4. Current transient of Fig. 3 plotted as functions of t^2 and t^3.

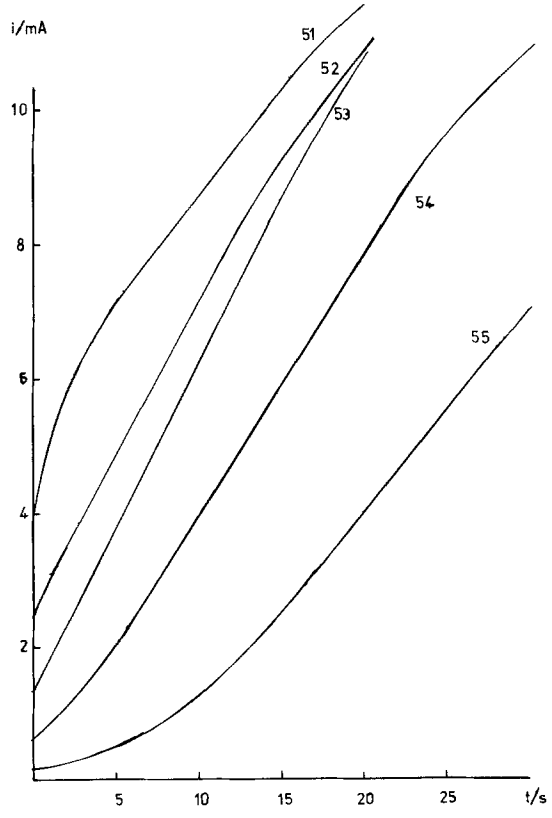

Fig. 5. Current–time transients at 340 mV. Nucleation at 600 mV: 51, 1 s; 52, 0.5 s; 53, 0.2 s; 54, 0.1 s; 55, 0 s; $[F^-] = 0$.

3.2. *Fluoride-containing solutions*

3.2.1. Potentiostatic transients. It was immediately apparent that the addition of fluoride to the electrolyte retarded the overall growth rate at a given potential, as illustrated by the transients for the nucleation step at 600 mV of Fig. 11. At 340 mV with an F^- concentration of about 1.0×10^{-2} M the current rose slowly and the linear i–t^3 plot of Fig. 12 was obtained for specimen 21. At higher F^- concentrations ($2–4 \times 10^{-2}$ M) deposition was insignificant at 340 mV, during the time periods considered here, unless a prior nucleation step was used. To obtain Fig. 13, nuclei were grown in the absence of fluoride for 30 s at 340 mV, the potential was stepped back to 0 mV for 20 s whilst fluoride was added to the solution, and then growth was continued at 340 mV.

In a series of experiments with a nucleation step of varying length, apparently linear i–t^2 relationships were recorded (Fig. 14). The current densities involved were quite low. The effect of fluoride on the growth rate was also observed in Fig. 15 for specimens subjected to fairly long nucleation steps.

3.2.2. Size distributions of nuclei. As before, measurements were made on the specimens sub-

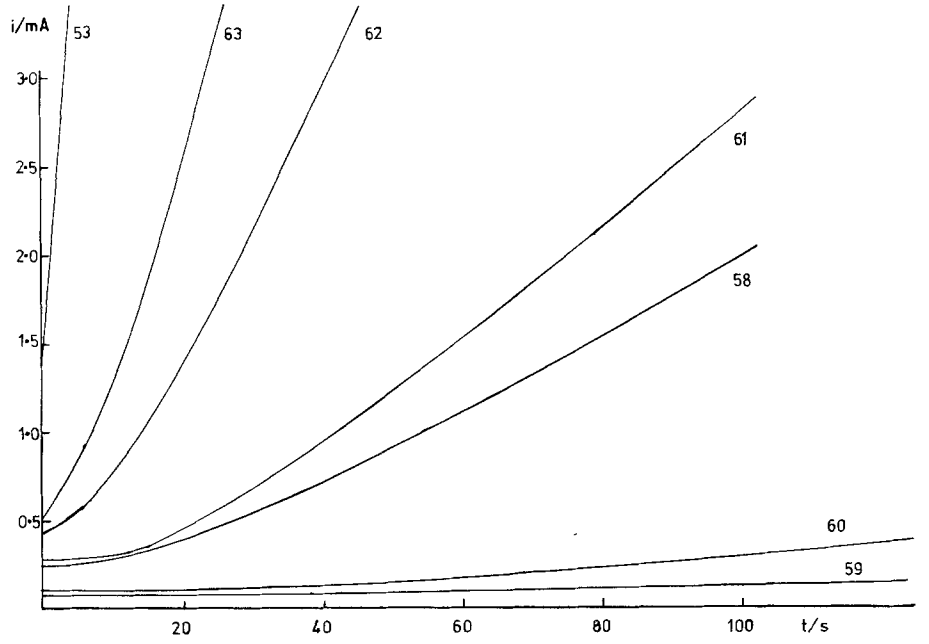

Fig. 6. Current–time transients after 0.2 s nucleation step at 600 mV. 59, 200 mV; 60, 225 mV; 58, 250 mV; 61, 275 mV; 63, 325 mV; 53, 340 mV.

jected to the transients just described. Fig. 16 refers to specimens nucleated for various short times (cf. Fig. 14), Fig. 17 to a specimen grown very slowly at 340 mV only (cf. Fig. 12), and Fig. 18 shows the time variation of the size distribution along the growth step for specimens nucleated for 10 s at 600 mV in 1.0×10^{-2} M fluoride, (cf. no. 43 in Fig. 15).

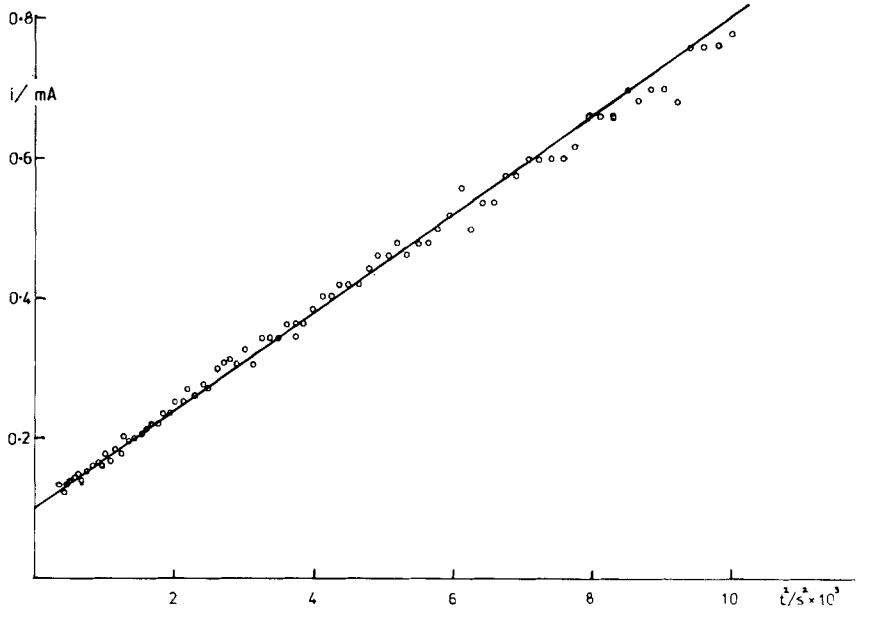

Fig. 7. Current transient for specimen 60 plotted as a function of t^2.

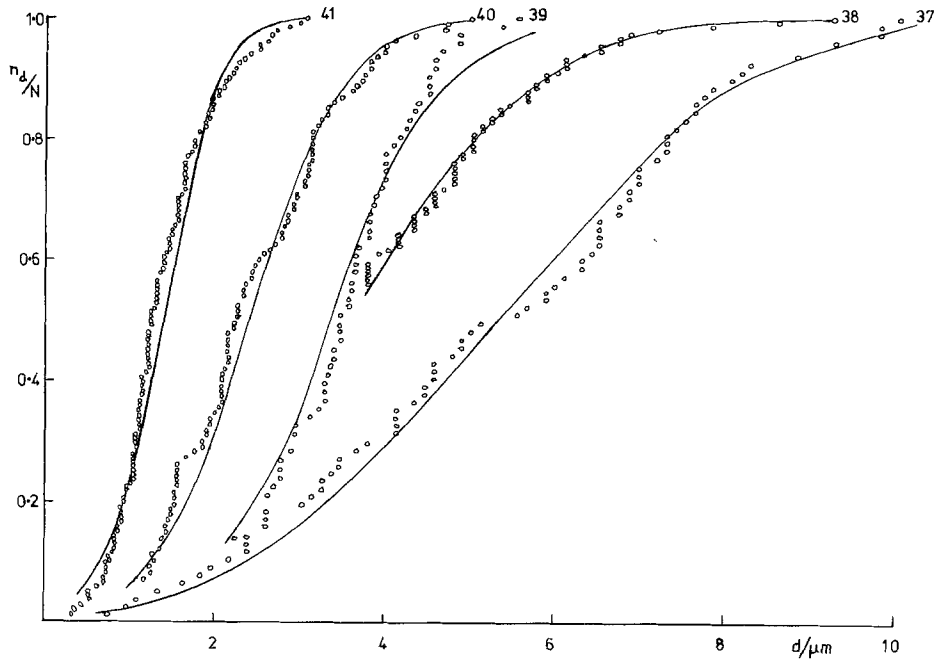

Fig. 8. Nuclei size distributions along the growth step at 340 mV after various polarization times: 41, 20 s; 40, 40 s; 39, 60 s; 38, 80 s; 37, 100 s; $[F^-] = 0$.

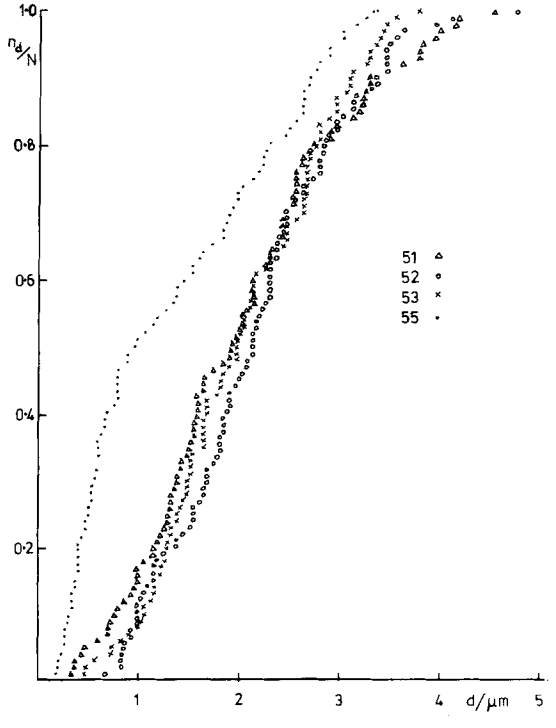

Fig. 9. Nuclei size distributions after 30 s growth at 340 mV for the specimens of Fig. 5.

3.3. *Surface density of nuclei*

For convenience, the deposition conditions and the measured surface densities of the lead dioxide nuclei are summarized in Table 1.

3.4. *Deposit morphology*

In the initial stages of growth the nuclei are spherical in appearance, but at higher magnification individual crystallites can be resolved, the surfaces of which are faceted. These take the form of multi-sided pyramids whose growth axes are directed towards the centre of the sphere. The number of crystallites on a nucleus of a given diameter depends markedly on the fluoride ion concentration. At high concentrations the number of crystallites is large and the spheres remain smooth, but with fluoride absent crystallite size becomes pronounced. The effect is illustrated by the micrographs of Fig. 19. After complete overlap of the nuclei, those pyramids aligned in the vertical direction continue to grow preferentially and thick deposits may then assume a columnar structure.

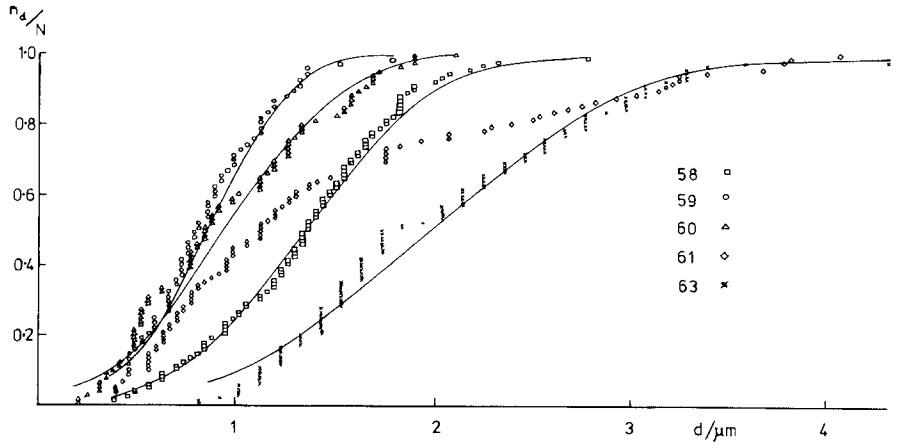

Fig. 10. Nuclei size distributions for the specimens of Fig. 6. Growth times are: 59, 60, 200 s; 58, 61, 100 s; 63, 50 s.

4. Discussion

4.1. *Idealized nucleation and growth*

Fleischmann and Thirsk [5] have presented a treatment of the nucleation and growth of electrodeposits under potentiostatic conditions. Assuming a uniform and constant current density at a spherical nucleus, they showed that the rate of increase of the radius is constant, and that the total current flowing into the nucleus depends on the square of its age. Before overlap becomes significant, two limiting cases, with the following criteria, are of interest.

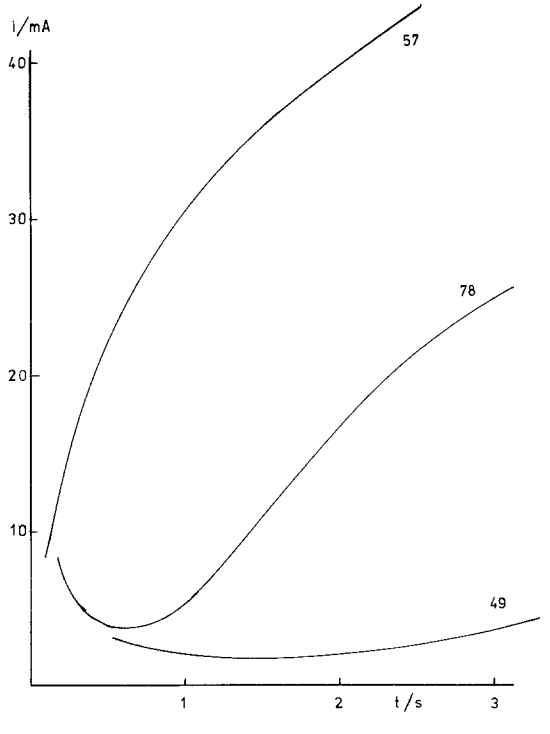

Fig. 11. Current–time transients at 600 mV showing effect of fluoride concentration: 57, $[F^-] = 0$; 78, $[F^-] = 2.0 \times 10^{-2}$ M; 49, $[F^-] = 4.0 \times 10^{-2}$ M.

(a) Progressive nucleation, where the rate of formation of new nuclei is constant. The total current, i, is proportional to t^3; the surface density of nuclei, N, is proportional to t; and the distribution of diameters is linear at any given time.

(b) Instantaneous nucleation, where all the nuclei are of the same age, might be induced by using a seeding or nucleation pulse at high potential followed by growth only at a lower potential. Then i depends on t^2; N is constant; and all the nuclei have the same radius.

From a practical point of view, the achievement of ideal behaviour would allow the possibility of controlling both the numbers of nuclei, and their size distribution. This would, in turn, enable some modification to be made of the adhesive and other properties of the deposit. Previous work may be examined to ascertain the extent to which the criteria, outlined above, have been realised. Fleischmann and Grenness [6] for example, found that the current was a linear function of t^3 during the deposition of ruthenium onto vitreous carbon, provided that an induction time was taken into account. The average diameter, and the numbers of nuclei increased linearly with time. The conditions for progressive nucleation therefore seem

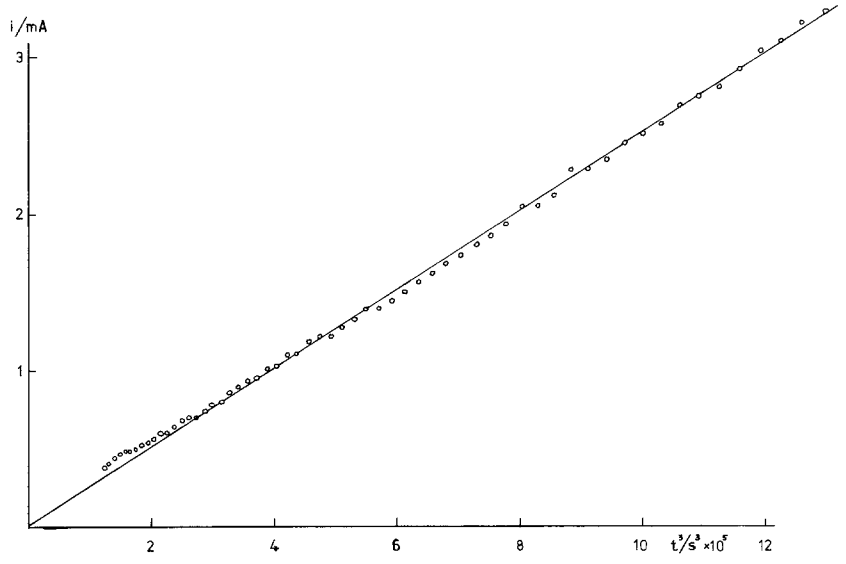

Fig. 12. Current transient at 340 mV for specimen 21 plotted as function of t^3. $[F^-] = 1.0 \times 10^{-2}$ M.

to have been satisfied, but i–t^2 plots were only linear, in the instantaneous nucleation experiments, if a negative induction time was assumed. The corresponding size distributions were not discussed. During deposition of lead dioxide on platinum,

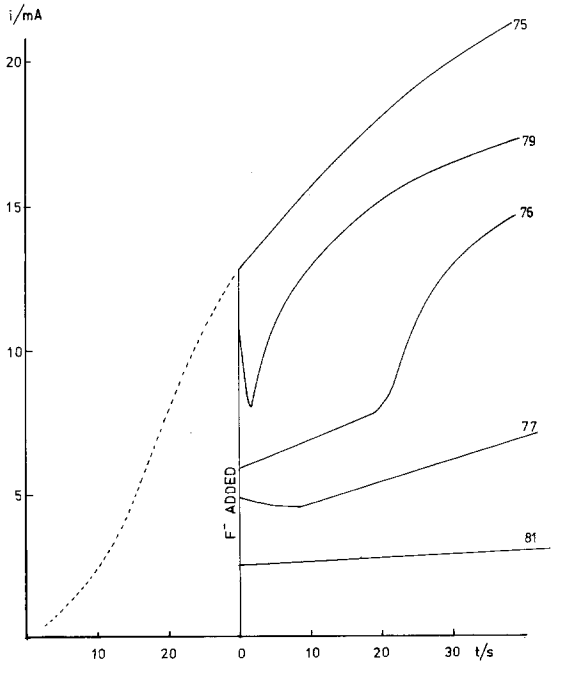

Fig. 13. Current transients at 340 mV with fluoride added after 30 s. Final concentrations: 75, $[F^-] = 0$; 79, $[F^-] = 0.5 \times 10^{-2}$ M; 81, $[F^-] = 3.0 \times 10^{-2}$ M; 76, $[F^-] = 1.0 \times 10^{-2}$ M; 77, $[F^-] = 2.0 \times 10^{-2}$ M.

Fleischmann and Liler [2] obtained the relevant linear plots for the two limiting situations, again by involving induction periods, but nuclei diameters were not measured. Similar results were obtained on tin oxide substrates by Laitinen and Watkins [7]. Apparently uniform crystals were produced under 'instantaneous' conditions, according to the published micrograph, although a size distribution was not measured. These results suggest that all the requirements for instantaneous nucleation are not easily achieved.

4.2. *Fluoride free solutions*

The relatively inert substrates used by the previous workers may be contrasted to the titanium wires used here, which are almost certainly covered with several monolayers of non-conducting oxide. The electrically resistant layer is probably responsible for the relatively low surface densities of nuclei, usually falling within the range 10^6–10^7 cm^{-2}, which are summarized in the histograms of Fig. 20. Fleischmann and Liler [2] estimated that the total number of active sites on platinum was about 10^9 cm^{-2}, and Laitinen and Watkins [7] concluded that tin oxide substrates were of similar activity. Examination of the present results for growth at 340 mV (specimens 37–41) indicates that the total number of nuclei does not increase with time. If anything the reverse happens, although this is probably due to coalescence. Saturation of the

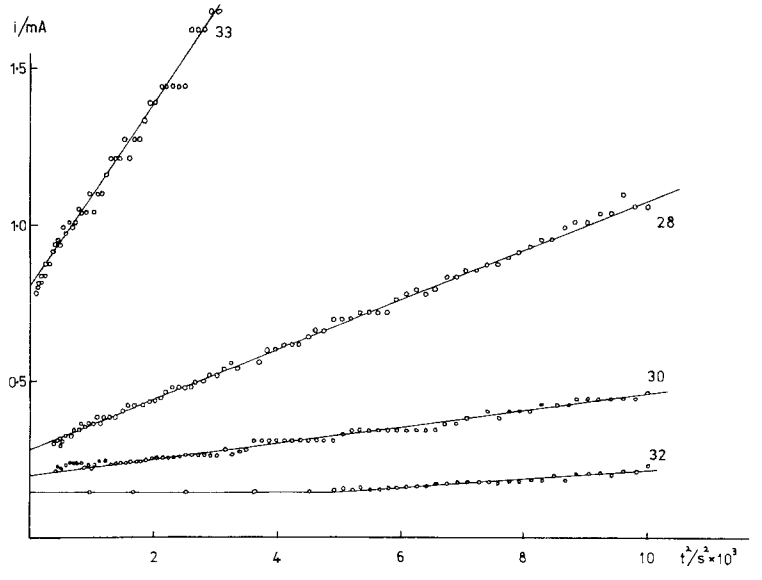

Fig. 14. Current transients at 340 mV, plotted as function of t^2. Nucleation step at 600 mV: 33, 2 s; 28, 1 s; 30, 0.5 s; 32, 0 s ($[F^-] = 1.0 \times 10^{-2}$ M).

active sites therefore seems to have occurred at an early stage, well before 20 s. The measured distribution of diameters of nuclei for various times of growth do not conform to the patterns described above. In fact the lines drawn in Fig. 8 (and in other diagrams) are those corresponding to normal distributions with means and standard deviations

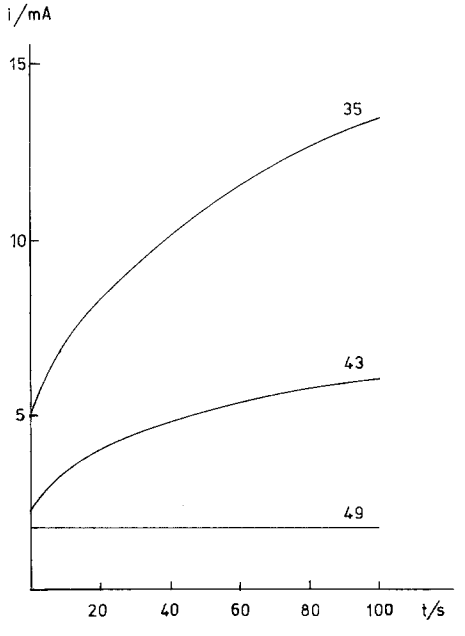

Fig. 15. Current transients at 340 mV after nucleation at 600 mV. 35, $t_{600} = 5$ s, $[F^-] = 0$; 43, $t_{600} = 10$ s, $[F^-] = 1.0 \times 10^{-2}$ M; 49, $t_{600} = 20$ s, $[F^-] = 4.0 \times 10^{-2}$ M.

calculated from the data points. These curves are seen to be a good representation of the experimental results. The diagram shows how the mean diameter of the nuclei increases regularly with time, so that the linear i–t^2 behaviour of Fig. 4 is readily accounted for, if an early saturation of the sites for nucleation is assumed.

The ratio of the standard deviation to the mean (σ/μ) is a quantity of some interest. Bindra *et al.* [8] have discussed the time variation of σ/μ for the observed currents in ensembles of transients at micro-electrodes. In a situation where nucleation is stochastic and growth is deterministic, they showed that σ/μ would tend to zero at long times, implying that the nuclei move towards a common size. In the present work, summarized in Table 2, the ratio is distributed around the values of 0.4 in the absence of fluoride, and 0.5 in fluoride containing solutions, without any evidence of time variation. This suggests a process in which the nuclei are enlarged in stages with growth ceasing at a particular crystal face and recommencing only after a renucleation. Such a model would be in accord with the observed physical appearance of the nuclei as exemplified in Fig. 19.

Specimens 50–55, used to investigate instantaneous nucleation, were subjected to short steps of varying lengths at 600 mV, followed by growth at 340 mV for 30 s. The expected t^2 dependence is not found, probably because overlap soon

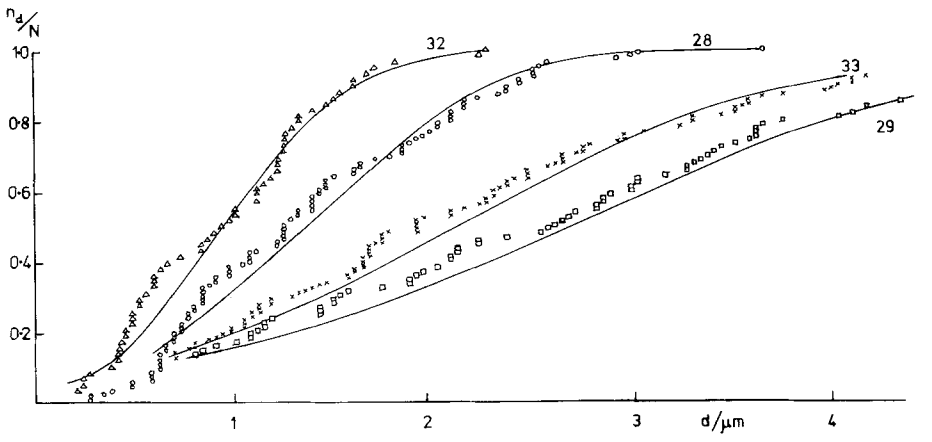

Fig. 16. Nuclei size distributions after 100 s growth at 340 mV for the specimens of Fig. 14 (29, $t_{600} = 5$ s).

becomes significant, but the transients show a progressive change in shape, from concave, through linear, to convex, as the length of the nucleation step is increased. The curves are very similar to those of comparable experiments on γ-MnO_2 deposition published by Fleischmann, Thirsk and Tordesillas [9]. They concluded that it would not be possible to manipulate the length of the pre-growth step in order to control or to estimate the surface density of the nuclei, and the same conclusion applies here. In fact the growth step transients in Fig. 5 converge after sufficiently long times, and even after 30 s the parameters describing the nuclei are practically identical on specimens 51–54. This convergence of behaviour is most likely due to the smoothing out, by the stochastic nature of the subsequent growth process, of any initial differences in the activities of the nuclei formed in the pre-growth step. At the same time the formation of a strictly uniform size distribution is prevented.

Specimens 58–63, which were used to demonstrate the effect of potential on the growth step, again have size spectra of the normal type, and under conditions of no overlap, i–t^2 behaviour was observed (59 and 60). The distribution for the nuclei on specimen 61 is unusual in that the point of inflexion is significantly displaced from the median towards lower values, giving a convex shape over a wide range. Sample 55 is similar, and both are better fitted by log-normal distributions. Values of σ/μ in Table 2 are seen to be anomolously high. Other specimens (e.g. 28, 33, and 44) show this behaviour to some extent and are best

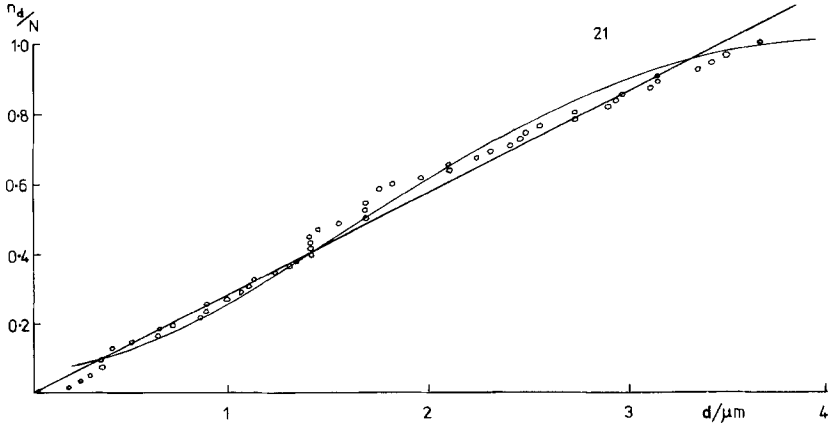

Fig. 17. Nuclei size distribution for specimen 21 after 110 s growth at 340 mV.

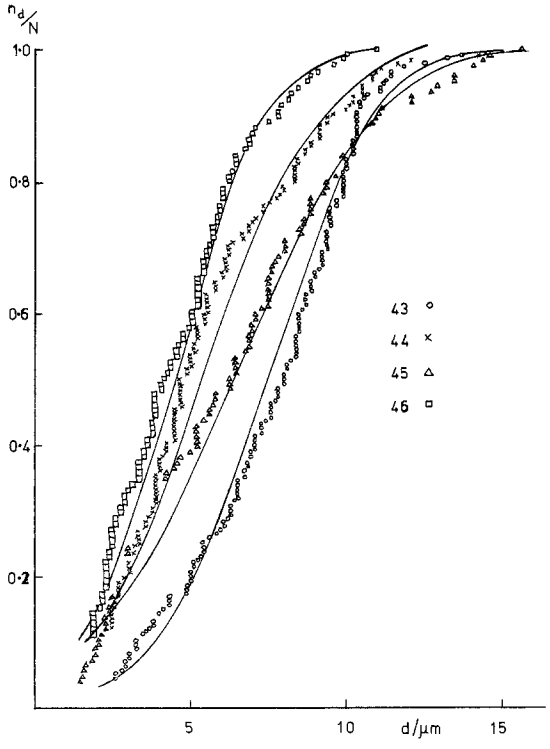

Fig. 18. Nuclei size distributions after 10 s nucleation step 600 mV followed by growth at 340 mV. 46, 40 s; 45, 60 s; 44, 80 s; 43, 100 s ($[F^-] = 1.0 \times 10^{-2}$ M).

fitted by log-normal curves at low nuclei diameters, although the normal curve is usually the better at high values.

4.3. *Effects of added fluoride*

Whilst Figs. 11 and 13 clearly show that fluoride ions significantly retard the overall growth rate of lead dioxide, it is of interest to establish whether this is due to a decrease in either the numbers of nuclei, or the current density at individual particles, or both. The results taken as a whole, summarized in the histograms of Fig. 20, indicate that the nuclei density is reduced by a factor of 2–3 in the presence of 10^{-2} M fluoride ions. The specific experiments on specimens 28–33 and 50–55, which were performed under comparable conditions of potential programming in the two solutions, support this conclusion. To assess the effect on the actual current density at the lead dioxide surface, it is necessary to work on an equivalent area basis. This has been done by performing the summation of the diameters $\sum_N d^2$, over the N nuclei in a given sample. The relative

Table 1

$[F^-] = 0$					$[F^-] = 1.0 \times 10^{-2} M$				
Specimen	*Nucleation*		*Growth time at 340 mV*	*Nuclei density* (10^{-6} cm^{-2})	*Specimen*	*Nucleation*		*Growth time at 340 mV*	*Nuclei density* (10^{-6} cm^{-2})
	E	*t*				*E*	*t*		
37	–		100	2.0	10	–		200	0.89
38	–		80	4.45	11	–		300	1.77
39	–		60	4.44	12	–		100	0.97
40	–		40	7.0	13	–		150	1.64
41	–		20	5.72	17	450	10	50	6.96
51	600	1	30	7.5	18	450	1	100	4.8
52	600	0.5	30	7.44	19	450	2	80	5.0
53	600	0.2	30	9.98	20	450	5	50	3.29
54	600	0.1	30	10.6	21	–		110	4.5
55	–		30	9.65	22	450	5	140	3.6
58	600	0.2	(at 250 mV) 100	11.6	26	450	5	140	4.97
59	600	0.2	(at 200 mV) 200	4.24	28	600	1	100	3.35
60	600	0.2	(at 225 mV) 200	4.8	29	600	5	100	3.0
61	600	0.2	(at 275 mV) 100	5.4	30	600	0.5	100	3.4
63	600	0.2	(at 325 mV) 50	4.78	31	600	0.2	100	3.66
					32	–		100	1.84
					33	600	2	100	3.93
					43	600	10	100	1.41
					44	600	10	80	1.64
					45	600	10	60	0.84
					46	600	10	40	1.78

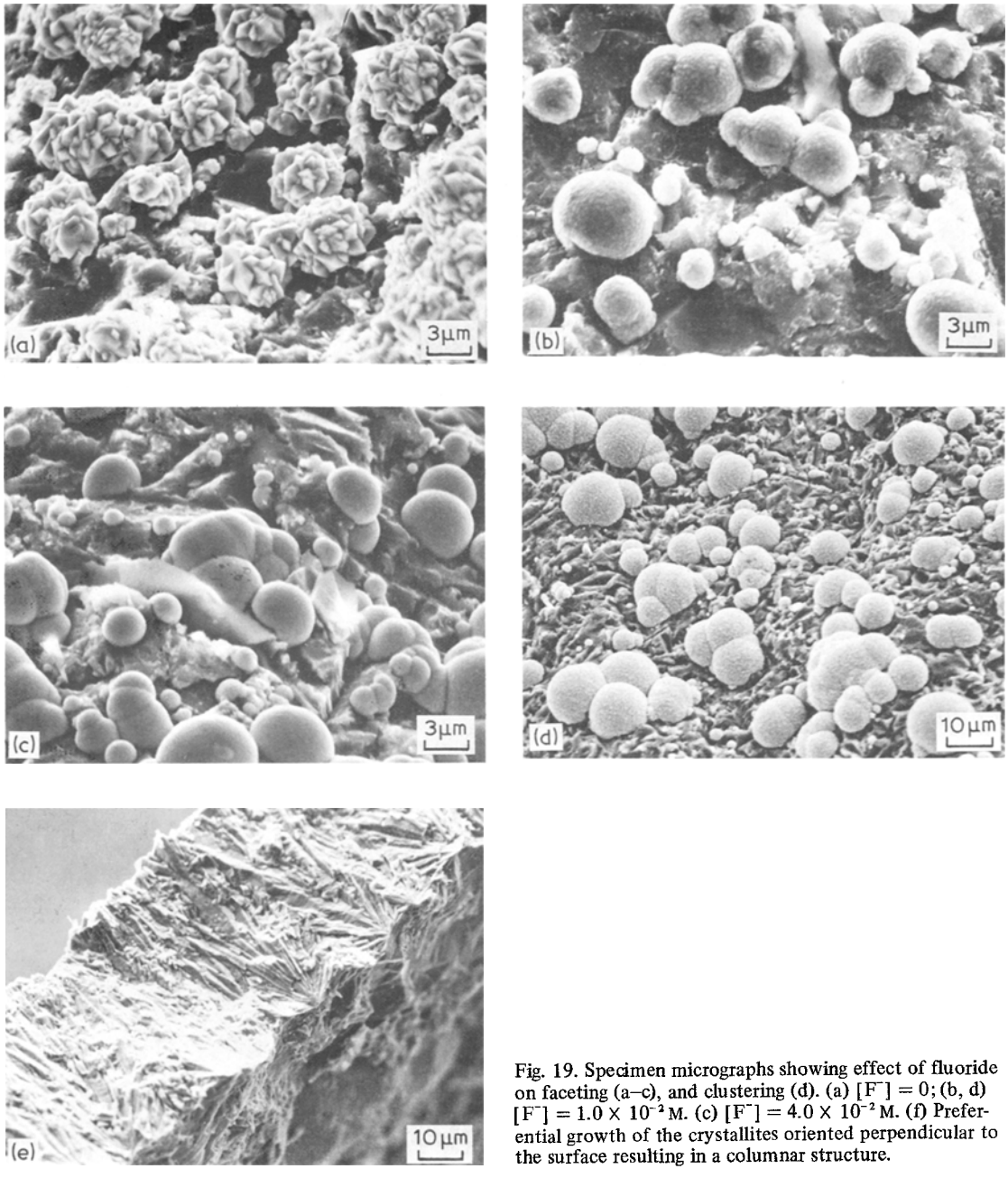

Fig. 19. Specimen micrographs showing effect of fluoride on faceting (a–c), and clustering (d). (a) $[F^-] = 0$; (b, d) $[F^-] = 1.0 \times 10^{-2}$ M. (c) $[F^-] = 4.0 \times 10^{-2}$ M. (f) Preferential growth of the crystallites oriented perpendicular to the surface resulting in a columnar structure.

nuclei area, A_N, is then calculated by assuming hemispherical geometry, neglecting overlap, and dividing by the appropriate substrate area. Hence

$$A_N = \tfrac{1}{2}\pi \sum_N d^2/\text{substrate area.}$$

In Fig. 21 the final currents for specimens grown at 340 mV in the presence and absence of fluoride, are plotted as functions of A_N. At low values of A_N a linear relationship exists, as expected, and the growth retarding effect of fluoride is demonstrated. At high A_N, the overlap of nuclei becomes more significant, and the current density tends towards a limiting value.

The action of fluoride may be considered initially by discussing the concept of an induction period for nucleation. In the present experiments,

Table 2. Parameters of nuclei distributions

$[F^-] = 0$				$[F^-] = 1.0 \times 10^{-2} M$			
Specimen	*Mean diameter* (μm)	*Standard deviation* (μm)	*Standard deviation/mean* (σ/μ)	*Specimen*	*Mean diameter* (μm)	*Standard deviation* (μm)	*Standard deviation/mean* (σ/μ)
37	5.35	2.35	0.44	10	3.42	1.53	0.45
38	3.64	1.81	0.50	11	5.67	2.35	0.42
39	3.39	1.07	0.31	12	1.32	0.44	0.33
40	2.42	0.93	0.38	13	1.53	0.61	0.40
41	1.37	0.56	0.41	17	2.16	0.58	0.27
51	1.87	0.90	0.48	18	1.28	0.84	0.65
52	1.98	0.79	0.40	19	1.16	0.72	0.62
53	2.01	0.78	0.39	20	0.80	0.57	0.72
54	2.11	0.84	0.40	21	1.47	0.87	0.58
55	1.28	0.93	0.73	22	1.44	0.82	0.57
50	2.68	0.86	0.32	26	1.64	1.05	0.64
58	1.45	0.56	0.39	28	1.41	0.72	0.52
59	0.90	0.36	0.40	29	2.65	1.61	0.61
60	1.04	0.51	0.49	30	1.44	0.72	0.50
61	1.56	1.03	0.67	31	1.17	0.53	0.45
63	2.12	0.85	0.40	32	0.94	0.50	0.52
				33	2.16	1.33	0.61
				43	7.53	2.69	0.36
				44	5.46	2.90	0.53
				45	6.41	3.50	0.54
				46	4.51	2.26	0.51

and in those of previous workers [2, 7] it is observed that in most of the measured transients, and especially in those with short or zero length nucleation pulses, the current passes through a shallow minimum. The time period involved is too long for the initial decay to represent double layer charging, and it has been suggested that a complete or partial layer of lead dioxide or of adsorbed lead ions must be deposited before growth can commence. Alternatively the delay

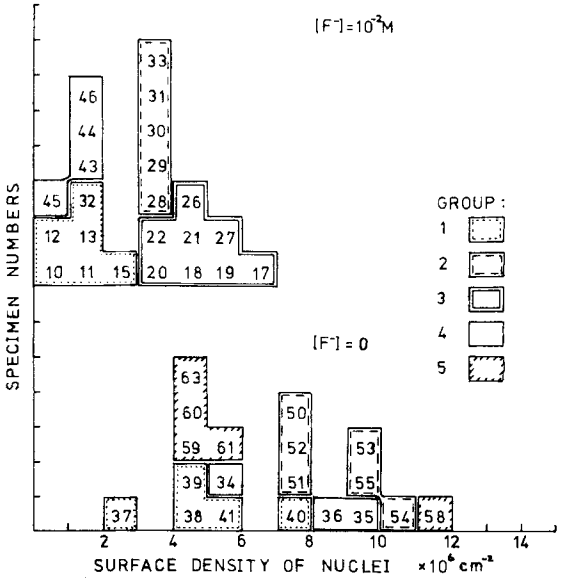

Fig. 20. Histograms showing the surface density of nuclei. Group 1: growth at 340 mV. Group 2: short nucleation step at 600 mV + growth at 340 mV. Group 4: long nucleation step at 600 mV + growth at 340 mV. Group 5: 0.2 s nucleation at 600 mV + growth at various potentials.

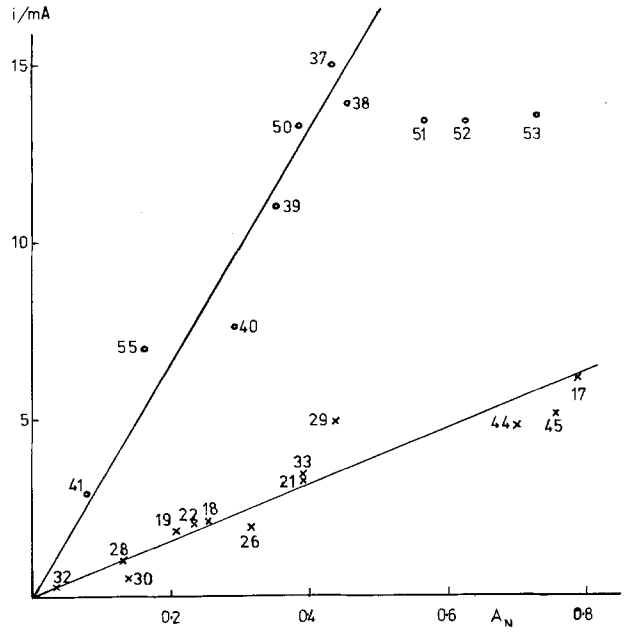

Fig. 21. Total current as a function of relative nuclei area. ○ $[F^-] = 0$; ×, $[F^-] = 1.0 \times 10^{-2}$ M.

enables the nucleus to exceed the critical size. It is often necessary to invoke an induction period when linearizing the dependence of i on t^3. A competitive adsorption of fluoride ions could inhibit the formation of the pre-adsorbed layer or the critical nucleus, and hence reduce the surface density of viable nuclei. Similar considerations might well be applicable to the growth process, especially in view of the proposed stochastic model, since fluoride adsorption onto the surfaces of the growing crystallites could contribute to the cessation of growth, and also inhibit subsequent renucleation. Two further observations may be encompassed by this model, namely the increase in the parameter σ/μ, given in Table 2, and also the increase in the degree of faceting or in the number of crystallites in a nucleus of given size in fluoride containing solutions. Both of these trends would be predicted in situations where the growth is interrupted and recommenced more frequently than in the reference state where interfering agents such as fluoride are absent.

It has been suggested [10] that fluoride might activate titanium substrates by a depassivation mechanism. The present results do not support this hypothesis, and preliminary experiments performed in this laboratory showed little or no effect of fluoride ion on the anodic oxidation of titanium at these potentials.

The slower growth patterns, brought about by the addition of fluoride may produce conditions more amenable to progressive nucleation. On specimen 21 the distribution of diameters (Fig. 17) could be interpreted either as linear or as normal with fairly high variance. The fact that a linear i–t^3 relation was obtained (Fig. 12) seems to indicate that the nucleation process was continuous in this case. (Complications due to overlap were absent).

The remaining experiments on specimens 28–33 and 43–46 consisted of attempts to achieve instantaneous nucleation using a seeding pulse of varying length at 600 mV. In the former group the linear i–t^2 plots of Fig. 14 were obtained with short pre-growth steps of less than 5 s duration. The nuclei diameters after 100 s growth conform fairly well to normal distributions (Fig. 16) with higher variance than the corresponding set in fluoride free solutions (specimens 51–54). The mean diameter increases with nucleation time at 600 mV, but the surface density of nuclei is fairly constant. With longer pre-treatment steps significant growth occurs at both potentials and nuclei overlap is present at an early stage.

On some of the specimens in these particular experiments clustering of the nuclei seems to occur. This leads to a somewhat patchy appearance with strings or groups of nuclei growing together with significant overlap, whilst on other parts of the surface the titanium substrate has a

lower density of nuclei. An example is given in Fig. 19d. The phenomenon may be associated with the occurence of the log-normal type of distribution as on specimen 28. One could predict that the adhesion of thick deposits grown from such samples, would be suspect.

5. Conclusions

The experimental results of the nucleation of lead dioxide on titanium wires have been interpreted in terms of the ideal behaviour expected for the extreme cases of progressive and instantaneous nucleation. To explain the results, and especially the observed size distributions, more completely, a stochastic growth model has been adopted. The following conclusions are made:

1. In the absence of fluoride it is difficult to observe progressive nucleation since the available sites appear to become rapidly saturated.

2. In these circumstances i–t^2 plots may be linear but the nuclear diameters depart from uniformity and instead have a normal distribution. The mean size increases regularly with time.

3. Controlled nucleation pulses cannot be used to achieve a uniform size distribution because of the stochastic growth process. It is also difficult to control the numbers of nuclei.

4. Fluoride ions decrease the surface density of nuclei, and also retard the growth rate at the lead dioxide surface.

5. In the initial stages the nuclei retain a smooth spherical appearance in fluoride containing solutions. Larger crystallites develop in the absence of fluoride.

6. Progressive nucleation is more readily established under the conditions of reduced growth rate brought about by fluoride additions.

7. Clustering phenomena may appear, especially in fluoride solutions.

The results have been further discussed by considering the competitive adsorption of fluoride ions on the pre-nucleation layer and on the growing lattice.

References

[1] G. H. Kelsall, Electricity Council Research Centre Report, N1060, June (1977).
[2] M. Fleischmann and M. Liler, *Trans. Farad. Soc.* **54** (1958) 1370.
[3] M. Fleischmann and H. R. Thirsk, *Electrochim. Acta* **1** (1959) 146.
[4] A. P. King, Electricity Council Research Centre Report, M1134 April (1978).
[5] M. Fleischmann and H. R. Thirsk, 'Advances in Electrochemistry & Electrochemical Engineering', Vol. 3 (edited by P. Delahay) Interscience, New York (1963) p. 123.
[6] M. Fleischmann and M. Grenness, *Trans. Farad. Soc.* **68** (1972) 2305.
[7] H. A. Laitinen and N. H. Watkins, *J. Electrochem. Soc.* **123** (1976) 804.
[8] P. Bindra, M. Fleischmann, J. W. Oldfield and D. Singleton, *Disc Farad. Soc.* **56** (1973) 180.
[9] M. Fleischmann, H. R. Thirsk and I. M. Tordesillas, *Trans. Farad. Soc.* **58** (1962) 1865.
[10] M. J. Mandry and G. Rosenblatt, *J. Electrochem. Soc.* **119** (1972) 29.